Magnetization tunneling in Mn-12 and Mn-4 single-molecule magnets

Magnetization tunneling in Mn12 and Mn4 single-molecule magnets

J. Yoo, E. M. Rumberger, D. N. Hendrickson, A. Yamaguchi, H. Ishimoto et al.

Citation: J. Appl. Phys. **91**, 7155 (2002); doi: 10.1063/1.1448785
View online: http://dx.doi.org/10.1063/1.1448785
View Table of Contents: http://jap.aip.org/resource/1/JAPIAU/v91/i10
Published by the AIP Publishing LLC.

Magnetization tunneling in Mn_{12} and Mn_4 single-molecule magnets

J. Yoo, E. M. Rumberger, and D. N. Hendrickson
Department of Chemistry and Biochemistry-0358, University of California at San Diego, La Jolla, California 92093-0358

A. Yamaguchi and H. Ishimoto
Institute for Solid State Physics, The University of Tokyo, 7-22-1 Roppongi, Minatoku, Tokyo 106-8666, Japan

E. K. Brechin and G. Christou
Department of Chemistry, University of Florida, Gainesville, Florida 32611-7200

The quantum mechanical tunneling of the direction of magnetization is discussed for several examples of single-molecule magnets (SMMs). SMMs are molecules that function as nanomagnets. Magnetization tunneling is described for two crystallographically different forms of $[Mn_{12}O_{12}(O_2CC_6H_4\text{-}p\text{-}Me)_{16}(H_2O)_4]\cdot$solvate. The two Mn_{12} complexes are isomers, differing both in the positioning of the H_2O and carboxylate ligands and also in the orientations of the Jahn-Teller elongation at the Mn^{III} ions. The magnetization vs magnetic field hysteresis loops are quite different for the two isomeric Mn_{12} complexes. Frequency-dependent ac magnetic susceptibility and dc magnetization decay data are presented to characterize the magnetization relaxation rate vs temperature responses of two mixed-valence Mn_4 complexes. In both cases the Arrhenius plot of the logarithm of the magnetization relaxation rate vs the inverse absolute temperature shows a temperature-dependent region as well as a temperature-independent region. [DOI: 10.1063/1.1448785]

I. INTRODUCTION

It was discovered in 1993 that

$$[Mn_{12}O_{12}(O_2CMe)_{16}(H_2O)_4]\cdot 4H_2O\cdot 2MeCOOH \quad (1)$$

functions as a nanoscale magnet.[1,2] Such a molecule has been called[3] a single-molecule magnet (SMM). There has been considerable interest in the magnetic properties of complex **1**,[4] which has an $S=10$ ground state split by axial zero-field splitting ($D\mathbf{S}_Z^2$, where $D=-0.5\ \mathrm{cm}^{-1}$). In 1996, it was reported[5,6] that complex **1** exhibits quantum mechanical tunneling of the direction of magnetization. The number of known single-molecule magnets is limited. Polynuclear metal complexes with the composition $Mn_4^{IV}Mn_8^{III}$, $Mn_4^{IV}Mn_7^{III}Mn_1^{II}$, $Mn^{IV}Mn_3^{III}$, $Mn_2^{III}Mn_2^{II}$, V_4^{III}, Fe_8^{III}, and Fe_4^{III}, have been identified as SMM's.

Each SMM functions as a superparamagnet as a result of having a large-spin ground state with appreciable magnetoanisotropy. At temperatures below the ''blocking temperature'' the magnetic moment of a SMM changes sluggishly from ''spin up'' to ''spin down.'' It is important to emphasize that the SMM phenomenon arises from the behavior of individual isolated molecules.

A SMM has a potential-energy barrier for reversal of its magnetic moment. It has been found that, in addition to thermal activation of each SMM over the barrier, the reversal of the direction of magnetization also occurs via quantum mechanical tunneling through the barrier.[4] In this paper we will discuss some recent observations on SMM's that are manifestations of magnetization tunneling.

II. EXPERIMENTAL RESULTS

The occurrence of magnetization tunneling is discussed for two $Mn_4^{IV}Mn_8^{III}$ and two $Mn_2^{III}Mn_2^{II}$ complexes. The complexes have the following formulas:

$$[Mn_{12}O_{12}(O_2CC_6H_4\text{-}p\text{-}Me)_{16}(H_2O)_4]\cdot(HO_2CC_6H_4\text{-}p\text{-}Me), \quad (2)$$

$$[Mn_{12}O_{12}(O_2CC_6H_4\text{-}p\text{-}Me)_{16}(H_2O)_4]\cdot 3H_2O, \quad (3)$$

$$[Mn_4(OAc)_2(pdmH)_6(H_2O)_4](ClO_4)_2, \quad (4)$$

$$[Mn_4(hmp)_6Br_2(H_2O)_2]Br_2\cdot 4H_2O. \quad (5)$$

In the case of complex $\mathbf{4}\cdot 2MeCN\cdot Et_2O$, the cation sits on a planar Mn_4 rhombus that is mixed-valent $Mn_2^{III}Mn_2^{II}$. This solvated complex readily loses acetonitrile to give complex **4** that has an $S=8$ ground state. Complex **5** consists of a planar Mn_4 rhombus and has a $S=9$ ground state.

Complexes **2** and **3** have the well known $[Mn_{12}O_{12}(O_2CR)_{16}(H_2O)_4]$ structure as has been reported[2,3] previously for the benzoate ($R=-C_6H_5$) and propionate ($R=-CH_2CH_3$) complexes. As a result of the different solvate molecules in the two crystals, complex **2** crystallizes in the $C2/c$ space group, whereas complex **3** crystallizes in the $I2/a$ space group. Even though both of these complexes have the same ligands on the Mn_{12} complexes, there are two significant differences in the molecular structures of the Mn_{12} molecules in **2** and **3**. First, complexes **2** and **3** differ in the positioning of the four H_2O ligands. The two Mn_{12} complexes are geometrical isomers with two different positionings of the H_2O and $^-O_2CC_6H_4\text{-}p\text{-}Me$ ligands. Complexes **2** and **3** have one other very important difference in their struc-

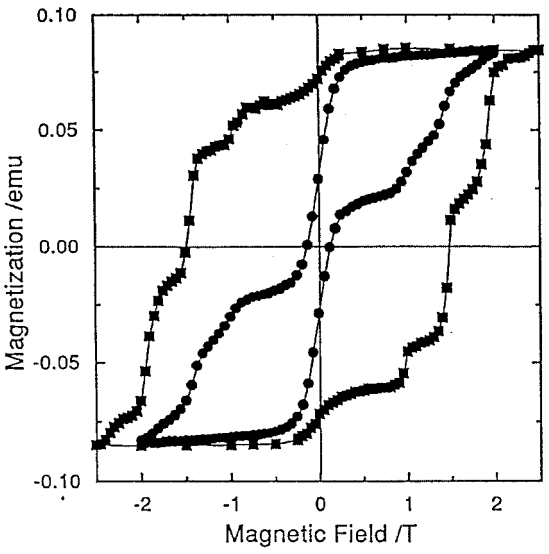

FIG. 1. Plots of magnetization vs external magnetic field for $[Mn_{12}O_{12}(O_2CC_6H_4\text{-}p\text{-}Me)_{16}(H_2O)_4]\cdot 3H_2O$ [(■), complex 3] and $[Mn_{12}O_{12}(O_2CC_6H_4\text{-}p\text{-}Me)_{16}(H_2O)_4]\cdot(HO_2CC_6H_4\text{-}p\text{-}Me)$ [(●), complex 2] at 1.90 K. Six small crystals (2.2 mg) of complex 2 were oriented in a frozen eicosane matrix so that the external magnetic field is parallel to the principal axis of magnetization. Five crystals (1.2 mg total) of complex 3 were oriented.

tures. Each Mn^{III} ion experiences a Jahn-Teller (JT) elongation. All of the JT elongation axes in the hydrate complex **3** are roughly parallel and perpendicular to the plane of the disklike $Mn_{12}O_{12}$ core. For complex **2**, however, one JT axis is abnormally oriented towards a core O^{2-} ion.

Complexes **2** and **3** have $S=10$ ground states, where the combination of a large spin and anisotropy leads to a potential-energy barrier for reversal of the direction of magnetization. Zero-field interactions split the $S=10$ state into the $M_s=\pm 10,\pm 9,\pm 8,...,\pm 1,0$ levels. The $M_s=-10$ state can be viewed as the ''spin up'' state and the $M_s=+10$ state as the ''spin down'' state. The double-well diagram of Fig. 1 shows how the potential energy of one molecule changes as it reverses its direction of magnetization from ''spin up'' to ''spin down.'' The potential-energy barrier is given as $U=|DS_z^2|$, where DS_z^2 gauges the axial zero-field splitting in the $S=10$ ground state.

Since complexes **2** and **3** have barriers for changing their magnetic moments from ''spin up'' to ''spin down,'' it is informative to examine the change in the magnetization of a sample as an external field is changed. For an oriented sample, steps can be seen at regular intervals of magnetic field in the magnetization hysteresis loop of a SMM. These steps result from a quantum mechanical tunneling of the magnetization.[5,6] Oriented samples of complexes **2** and **3** were prepared by suspending a few small crystals of either complex in an eicosane wax cube.

Figure 1 shows the magnetization hysteresis data measured for complex **3** at 1.90 K. Magnetization hysteresis loops were determined in the 1.72–2.50 K range. The coercive magnetic field and consequently the area enclosed within a hysteresis loop increase as the temperature is decreased. At 1.72 K the coercive magnetic field for complex **7** is ≈2 T.

Magnetization hysteresis loops were also measured for the oriented eicosane cube of complex **2** at the temperatures of 1.72, 2.20, 2.00, 1.90, and 1.80 K (the 1.90 K data are shown in Fig. 1). The hysteresis loops for complex **2** look quite different than those for complex **3**. When the external field is reduced from +2.5 T to zero, the magnetization falls off dramatically. The coercive fields are considerably less for complex **2** than for complex **3**. These two *p*-methylbenzoate Mn_{12} complexes experience quite different kinetic barriers for reversal of magnetization. It must be emphasized that the sweep rate for all the loops was 25 Oe/s.

From the hysteresis loop data it is clear that the *p*-methylbenzoate complex **2** has an appreciably greater rate of magnetization relaxation than does isomeric complex **3**. This can be quantified by analyzing the frequency dependencies of the out-of-phase ac susceptibilities. Ac susceptibility data were collected at 8 different frequencies from 1.0 Hz to 1512 Hz for complex **3**. From the peaks in the χ_M'' vs temperature plots values of the magnetization relaxation time τ were determined at 8 temperatures. These data give a straight line Arrhenius plot of $\ln(1/\tau)$ vs the inverse absolute temperature $(1/T)$ for complex **3**. The data were least-squares fit to the Arrhenius equation to give the parameters of $\tau_0=7.7\times10^{-9}$ s and $U_{\text{eff}}=64$ K. A similar analysis of the frequency dependence of the ac data for complex **2** gives $\tau_0=2.0\times10^{-10}$ s and $U_{\text{eff}}=38$ K. The activation energy (U_{eff}) for reversal of the direction of the magnetization for complex **2** ($U_{\text{eff}}=38$ K) is considerably less than that ($U_{\text{eff}}=64$ K) for the isomeric complex **3**. The Mn_{12}-acetate complex **1** has been reported[4] to have a U_{eff} value of 62 K, very close to the value for complex **3**.

It is likely that the appreciably faster rate of magnetization tunneling observed for complex **2** compared to the isomeric complex **3** is due to the lower symmetry observed for complex **2**. This lowered symmetry would increase the rhombic zero-field splitting $[E(\mathbf{S}_x^2-\mathbf{S}_y^2)]$ in the $S=10$ ground state of complex **2** leading to an increase in the rate of magnetization tunneling.

Variable-field magnetization data have been fit to determine that complex **4** has an $S=8$ ground state[7,8] with $D/k_B=-0.358$ K. Ac magnetic susceptibility measurements were carried out by cooling the sample with a ^3He–^4He dilution refrigerator in the 0.04–3.5 K range. Eleven different ac frequencies were used in the 1.1–995 Hz range, which gave rates of magnetization reversal at 11 different temperatures. These relaxation data fit well to the Arrhenius equation to give an activation energy for magnetization reversal of $U_{\text{eff}}=17.3$ K with a pre-exponential factor of $\tau_0=2.54\times10^{-7}$ s. The thermodynamic barrier can be calculated to be $U=22.4$ K. As with other SMMs, it is expected that $U>U_{\text{eff}}$, for the reversal of magnetization not only involves a thermal activation over the potential-energy barrier, but also quantum tunneling of the direction of magnetization.

The most definitive data showing that complex **4** does reverse its magnetization direction by quantum tunneling were obtained by means of magnetization decay experiments. In a dc magnetization decay experiment the sample is

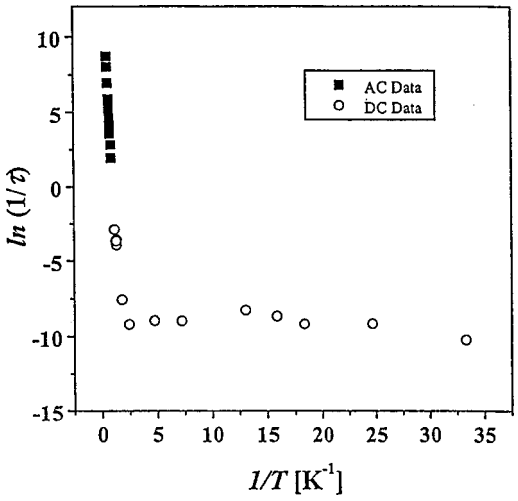

FIG. 2. Plot of the natural logarithm of the relaxation rate ($1/\tau$) vs the inverse absolute temperature for complex 4. The symbol (■) represents the data collected with the ac magnetic susceptibility technique, and the magnetization decay data are indicated by the symbol (○).

first cooled and maintained at a low temperature, after which it is subjected to a very small magnetic field. At low temperatures, only a small field is needed to achieve magnetization saturation. The field is then suddenly removed and the magnetization is measured as a function of time. Over time the magnetization decays from some initial value at time zero, defined as the time when the applied field becomes zero, to an equilibrium value.

Plots of magnetization vs time were measured in the 0.030–0.860 K range. These magnetization decay data were fit to a stretched exponential function. This gave a set of relaxation times at temperatures in the 0.030–0.860 K range. It was found that at temperatures above $\sim$ 0.5 K the magnetization relaxation time τ is temperature dependent.

The magnetization rate data obtained at higher temperatures for complex **4** with ac susceptibility measurements are combined with the dc magnetization decay rate data as an Arrhenius plot of $\ln(1/\tau)$ vs $1/T$ in Fig. 2. This is indeed a very revealing plot, for it can be seen at temperatures above $\sim$0.5 K the magnetization relaxation rate is temperature dependent with an activation energy of $U_{\text{eff}}=17.3$ K. However, at low temperatures below $\sim$0.5 K, the relaxation rate is clearly temperature independent, indicating that the magnetization relaxation below this temperature is occurring purely by a quantum tunneling phenomenon. Complex **4** tunnels between the $M_s=-8$ and $M_s=+8$ levels at a rate of approximately 1×10^{-4} s^{-1}.

Magnetization relaxation decay data were also collected for a sample of complex **5** in the 0.047–1.195 K range. This complex has an $S=9$ ground state. The decay data were least-squares fit to give relaxation rates in the above temperature range. These rates were combined with those obtained at higher temperatures by means of the ac susceptibility. At the higher temperatures the relaxation rate is temperature dependent with an activation energy of 15.8 K. At the lower temperatures we again see a temperature-independent rate of relaxation. This is surely attributable to ground state magnetization tunneling. The temperature-independent magnetization tunneling rate is 1×10^{-3} s^{-1} for complex **5**. Preliminary HFEPR data indicate that complex **5** experiences a larger rhombic zero-field splitting than does complex **4**. This would explain the faster rate of tunneling in complex **5**. Further experimentation is needed on these interesting tetranuclear manganese SMMs to understand in detail the mechanism of magnetization tunneling in these complexes.

ACKNOWLEDGMENT

D. N. H. and G. C. thank the National Science Foundation for support of this research.

[1] R. Sessoli, D. Gatteschi, and M. Novak, Nature (London) **365**, 149 (1993).
[2] R. Sessoli, H.-L Tsai, A. R. Schake, S. Wang, J. B. Vincent, K. Folting, D. Gatteschi, G. Christou, and D. N. Hendrickson, J. Am. Chem. Soc. **115**, 1804 (1993).
[3] S. M. J. Aubin, M. W. Wemple, D. M. Adams, H.-L. Tsai, G. Christou, and D. N. Hendrickson, J. Am. Chem. Soc. **118**, 7746 (1996).
[4] G. Christou, D. Gatteschi, D. N. Hendrickson, and R. Sessoli, MRS Bull. **25**, 66 (2000); I. Chiorescu, R. Giraud, A. G. M. Jansen, A. Caneschi, and B. Barbara, Phys. Rev. Lett. **85**, 4807 (2000); S. M. J. Aubin, Z. Sun, H. J. Eppley, E. M. Rumberger, I. A. Guzei, K. Folting, P. K. Gantzel, A. L. Rheingold, G. Christou, and D. N. Hendrickson, Inorg. Chem. **40**, 2127 (2001).
[5] J. R. Friedman, M. P. Sarachik, J. Tejada, and R. Ziolo, Phys. Rev. Lett. **76**, 3830 (1996).
[6] L. Thomas, F. Lionti, F. R. Ballou, D. Gatteschi, R. Sessoli, and B. Barbara, Nature (London) **383**, 145 (1996).
[7] J. Yoo, E. K. Brechin, A. Yamaguchi, M. Nakano, J. C. Huffman, A. L. Maniero, L.-C. Brunel, K. Awaga, H. Ishimoto, G. Christou, and D. N. Hendrickson, Inorg. Chem. **39**, 3615 (2000).
[8] J. Yoo, A. Yamaguchi, M. Nakano, J. Krzystek, W. B. Streib, L.-C. Brunel, H. Ishimoto, G. Christou, and D. N. Hendrickson, Inorg. Chem. **40**, 4604 (2001).